Composites Part B 79 (2015) 170–181

Contents lists available at ScienceDirect

Composites Part B

journal homepage: www.elsevier.com/locate/compositesb

Monomer casting nylon-6-b-polyether amine copolymers: Synthesis and properties

Sheng Xu, Lin Ye*

State Key Laboratory of Polymer Materials Engineering, Polymer Research Institute of Sichuan University, Chengdu, 610065, China

ARTICLE INFO

Article history:
Received 22 October 2014
Received in revised form
22 April 2015
Accepted 23 April 2015
Available online 1 May 2015

Keywords:
A. Thermoplastic resin
B. Fracture toughness
B. Mechanical properties
B. Rheological properties

ABSTRACT

MC nylon-6-b-polyether amine copolymers were prepared with macro-initiator based on amino-terminated polyether amine functionalized with isocyanate via in-situ polymerization. It was found that the introduction of polyether amine delayed the polymerization process of caprolactam by increasing apparent activation energy and pre-exponential factor, resulting in the decrease of molecular weight of nylon-6. The motion of molecular chain of the copolymers was easy because of the decreased hydrogen bonds and weakened inter-molecular forces. The physical entanglement of molecular chains of the copolymers was significant and strong which increased the entanglement density. Only the nylon-6 phase crystallized in the copolymers and the crystal grain size, spherulite size and crystallinity of the copolymers decreased. A small amount of γ crystal formed at high polyether amine content. The copolymers presented obvious strain hardening behavior in stress-strain curves and the loss factor dramatically increased while the glass transition temperature and storage module decreased. The fracture surface of the copolymers became rough and presented hairy structure, indicating that the toughening mechanism of the copolymers corresponded to the multi-layer crack extension mechanism.

1. Introduction

Monomer casting (MC) nylon-6 is a new type of engineering plastics, which is synthesized by anionic polymerization with caprolactam as the major raw material. Compared with ordinary nylon-6, it takes advantages of high molecular weight, high mechanical strength and excellent self-lubricating performance [1–4], and widely used to replace metallic materials for the production of gears, bearings and slide blocks [5].

However, MC nylon-6 presents a disadvantage in its low-notched impact strength at low temperature or low moisture content. It is not resistant to crack propagation, which often results in brittle failure. The inherent notch sensitivity of MC nylon-6 precludes its use in applications such as automotive fender, body panels, housing equipment and industrial appliances, which require high impact resistance. Many attempts have been made to improve the toughening properties of MC nylon-6 by blending soft component or adding plasticizing agents, such as UHMWPE powders, HPT (hexamethylphosphoric triamide) and so on. Zhang et al. [6] showed the UHMWPE powders treated by epoxy resin dispersed homogeneously in the nylon-6 matrix. The impact strength reached maximum values at 8 wt% UHMWPE powders content, and the wear resistance gets improved gradually. Wang et al. [7] prepared HPT toughened MC nylon-6 blend, which impact strength and elongation at break increased, and crystallinity decreased. Some researches attempted to toughen MC nylon-6 by preparing novel catalyst or activator with a multi-functional group [8] or copolymerized with other components. The copolymer methods [9] were applied widely because of simple technology, stable structure and evident toughness of materials. Cheng et al. [10] prepared MC nylon-6/dodecanoic lactam copolymers, which formed random copolymer and exhibited increasing impact strength; Petrov et al. [11] investigated block copolymers of MC nylon-6 with different polybutadiene contents, which showed a toughness of the block copolymers without significant changes in their melting temperatures, and exhibited micro-phase separation in the copolymers. However, as reported, most of the copolymers with phase or micro-phase separation showed a low tensile strength even though the impact toughness was improved.

Polyether amine with low molecular weight has been widely applied in many fields. It was used as an important raw material of polyurea elastomer and acted as a new hardener of epoxy resin.

* Corresponding author. Tel.: +86 28 85408802; fax: +86 28 85402465.
E-mail address: yelinwh@126.com (L. Ye).

http://dx.doi.org/10.1016/j.compositesb.2015.04.040
1359-8368/

However, in this work it is the first time to use the polyether amine as copolymerization component in MC nylon-6 matrix. Based on the addition reaction mechanism of substituting-urea, the polyether amine was terminated with isocyanate in each branched-chain and formed multi N-acyllactam chain-growing centers, and finally, the polymerization process was conducted and the copolymers grew with multi-branched molecular chains. The flexible structure of C—O—C bond in polyether amine molecular chain endowed the material with excellent toughness. Besides, unlike the simply blending with high molecular weight soft component [11], the phase separation phenomenon was difficult to occur due to the copolymerization method and low molecular weight of polyether amine. Thus, polyether amine is a good candidate as an organic toughening material. In this work, polyether amine with an average molecular weight of 2000 g/mol was consisted of propylene oxide chain structure and terminated with amino groups (abbreviation: POD). The effect of POD on reaction kinetics of caprolactam polymerization was studied, the molecular chain structure of the copolymers was characterized, and the toughening mechanism was explored in terms of FTIR, SEM, and crystallization and rheology analysis.

2. Experimental

2.1. Materials

The caprolactam monomer was supplied by China Petroleum and Chemical Co. Ltd., with a commercial grade product. NaOH (sodium hydroxide), as the catalyst with analytical purity was purchased from Kermel Chemical Reagent Co. Ltd. (Tianjin, China), and TDI (toluene-2, 4-diisocyanate), as the initiator, was purchased from Kelong Chemical Reagent Factory (Chengdu, China). Polyether amine with an average molecular weight of 2000 g/mol (POD) was purchased from Huntsman Polyurethanes Ltd. Guangzhou Branch (Guangzhou, China).

2.2. Synthesis and preparation

2.2.1. Synthesis of TDI-POD macro-initiator

TDI-POD macro-initiator was prepared at room temperature with a constant temperature bath. A flask was equipped with magnetic stirrer and charged with a certain quantity of TDI. POD liquid was slowly dropped with corresponding molar ratio. The reaction lasted for 2 h to make sure the reaction was completed. Then the TDI-POD macro-initiator was obtained.

2.2.2. Synthesis of MC nylon-6-b-POD copolymers

A proper quantity of caprolactam (CL) was put into a flask and heated to about 130 °C. After completely melting, the mixed melt was refluxed under vacuum for about 30 min to remove water in it. Then a proper amount of NaOH was added under dramatically stirring. The melt was refluxed under vacuum for another 30 min, and a certain quantity of TDI-POD macro-initiator was added. After quickly well mixed up, the melt was casted into a preheated mould at 160 °C. The reaction lasted for 40 min. The product of MC nylon-6-b-POD copolymer was then obtained.

2.3. Measurements

2.3.1. Reaction kinetics analysis

Caprolactam polymerization proceeded in the mould which was put in a thermal isolation oven. The reaction temperature during caprolactam polymerization was measured precisely with a TM-902C thermometer from Shanglong Electric Co. Ltd. (Shanghai, China), and the reaction kinetics was analyzed with the recorded reaction temperature.

2.3.2. ^1H NMR analysis

^{1}H NMR measurements of neat MC nylon-6 and MC nylon-6-b-POD copolymers were performed with Varian Inova-600 NMR spectrometer (Chesterfield of MI, USA) at room temperature. The test was operated with a frequency of 600 MHz and the solvent was trifluoroacetic acid-D (TFA-D). Before the test, the samples were purified.

2.3.3. FTIR analysis

The structure of the neat MC nylon-6 and MC nylon-6-b-POD copolymers was analyzed with a Nicolet-560 Fourier-transform infrared spectrometer (FTIR) (U.S.A). The scanning rate was 20 min^{-1}, and the differentiate rate was 4 cm^{-1}.

2.3.4. Viscosity average molecular weight

The viscosity average molecular weight of neat MC nylon-6 and MC nylon-6-b-POD copolymers was measured with an Ubbelohde viscometer. The formic acid was used as solvent of nylon-6 materials. According to ISO 307-1984, the specific viscosity can be calculated with the following formula.

$$\eta_{sp} = (t - t_0)/t_0 \tag{1}$$

where η_{sp} is the specific viscosity; t, the flow time of a polymer solution through a capillary tube of known diameter and length, and t_0 is the flow time of the pure solvent through the same capillary tube.

The intrinsic viscosity is described as the limit of the ratio between the specific viscosity (η_{sp}) and the polymer concentration (c), as the polymer concentration approaches zero.

$$[\eta] = \lim \eta_{sp}/c(c \to 0) \tag{2}$$

By measuring the intrinsic viscosity of polymer solutions, the polymer average molecular weight can be predicted through the Mark-Houwink empirical equation, as described by:

$$[\eta] = KM_\eta^\alpha \tag{3}$$

where $[\eta]$ is the intrinsic viscosity, K and a are the parameters that depend on the solvent/polymer pair and the value of $22.6^{*}10^{-3}$ and 0.82 were chosen respectively [12]. M_η is the viscosity average molecular weight of the polymer.

2.3.5. Non-isothermal crystallization DSC analysis

The non-isothermal crystallization of neat MC nylon-6 and MC nylon-6-b-POD copolymers was performed with a Netzsch 204 Phoenix differential scanning calorimetry (DSC) (Germany). The temperature scale of DSC was calibrated with indium. Granulated samples of about 10 mg were heated from ambient temperature to 250 °C at a constant rate of 10 °C/min under nitrogen atmosphere.

After holding for 5 min to eliminate the effect of the previous thermal history, the samples were cooled to ambient temperature at the same constant rate. The crystallinity ($X_{c,\ DSC}$) can be calculated with the following equation:

$$X_{c,\mathrm{DSC}} = [\Delta H_m/(w \cdot \Delta H_0)]^{*}100\% \tag{4}$$

where w is the mass fraction of each component; ΔH_m is the melting enthalpy of the samples and ΔH_0 is the balance melting enthalpy, i.e., the melting enthalpy of 100% crystallizing polymer, which is 230 J/g for MC nylon-6 [13,14].

2.3.6. X-ray diffraction analysis (XRD)

The XRD analysis of neat MC nylon-6 and MC nylon-6-b-POD copolymers was performed with a Rigaku D/max IIIB X-ray diffractometer (Japan) at room temperature. XRD data were collected from 5 to 40°.

2.3.7. Polarized light microscopy analysis (PLM)

The crystal morphology of neat MC nylon-6 and MC nylon-6-b-POD copolymers was observed with a Leitz Laborlux polarized light microscopy (PLM) (Germany).

2.3.8. Scanning electron microscopy analysis (SEM)

The morphology of the impact fractured surface of neat MC nylon-6 and MC nylon-6-b-POD copolymers was observed with a JEOL JSM-5900LV SEM (Japan). The operating voltage was 5 kV. The samples were ion beam sputter-coated with gold and the thin layer thickness was about 1–20 nm.

2.3.9. Dynamic rheological analysis

Rheological characterization of neat MC nylon-6 and MC nylon-6-b-POD copolymers was carried out at 250 °C on a rheometer (TA-AR2000ex, USA) with a 25 mm-parallel plate in a frequency range of 0.01–100 Hz and 1% strain value. The testing sample disks with a thickness of 1.5 mm and a diameter of 25 mm were prepared by compression-molding at 250 °C.

2.3.10. Dynamic mechanical analysis (DMA)

The dynamic mechanical analysis (DMA) of neat MC nylon-6 and MC nylon-6-b-POD copolymers was carried out by using a TA Instrument Q800 DMA (U.S.A). All the samples were measured with a bending mode at a heating rate of 3 °C/min and a frequency of 1 Hz. The sample size was 40*10*4 mm^3.

2.3.11. Mechanical properties

The tensile performance of neat MC nylon-6 and MC nylon-6-b-POD copolymers was measured with a 4302 material testing machine from Instron Co. (U.S.A), according to ISO 527-1993. The tensile test speed was 10 mm/min, and the sample length between bench marks was 25 ± 0.5 mm.

The notched charpy impact strength of neat MC nylon-6 and MC nylon-6-b-POD copolymers was measured with ZBC-4B impact testing machine from Xinsansi Co. (Shenzhen, China) according to ISO 179-1993 standards.

3. Results and discussion

3.1. Synthesis and structure of MC nylon-6-b-POD copolymers

The multi-armed TDI-POD macro-initiator was prepared based on the addition reaction of substituting-urea between the amino group of POD and the isocyanate group of TDI, and the reaction mechanism is shown in Scheme 1(a). MC nylon-6-b-POD was fabricated by means of cast moulding technique via the mechanism of anionic ring-opening polymerization, using NaOH as catalyst and the above TDI-POD as macro-initiator. The reaction mechanism of copolymers is shown in Scheme 1(b).

3.1.1. Reaction kinetics

The temperature–time relationship curves of MC nylon-6-b-POD copolymers with various POD content during the polymerization process are shown in Fig. 1(a). The polymerization process started when the caprolactam melt was cast into a preheated mould at 160 °C. Therefore, at first, the temperature of the reaction system decreased from mold temperature (160 °C) to caprolactam melt temperature (130 °C) and then increased gradually with time. In about 400–1200 s, the temperature of the reaction system tended to be stable, indicating of the end of the polymerization process. The equilibrium temperature was 20–30 °C higher than that of the initial mold temperature, indicating that the caprolactam polymerization process was an exothermic reaction.

As seen in Fig. 1(a), the reaction temperature of the neat MC nylon-6 which was initiated by TDI increased rapidly and the reaction process terminated in short time, while the reaction temperature of the copolymer system increased slowly by introduction of POD, indicating of relatively low initiation activity of TDI-POD macro-initiator. The heating-rate curves of the copolymers are shown in Fig. 1(b). The heating-rate of all copolymers increased first and then decreased with time, and reached maximum within 300–900 s. With the increase of POD content, the maximum heating-rate (R_{max}) decreased and the time corresponding to the maximum heating-rate (t_{max}) was significantly prolonged, as listed in Table 1.

As to an exothermic chemical reaction, the universal equation for studying the non-isothermal reaction kinetics can be stated as following [15]:

$$\mathrm{d}\alpha/\mathrm{d}t = (1-a)^n \cdot A \cdot e^{(-E/RT)} \tag{5}$$

where α is the reaction conversion rate; t is the reaction time; n is the reaction order; A is the pre-exponential factor; T is the reaction temperature; E is the apparent activation energy of the reaction and R is the gas constant with value of 8.314 J/(K mol).

Transforming Equation (5) into double-logarithmic form, the following universal equation for studying the non-isothermal reaction kinetics can be obtained:

$$\ln(\mathrm{d}a/\mathrm{d}t) = \ln A + n \cdot \ln(1-a) - E/RT \tag{6}$$

Polymerization reaction was conducted in a thermal isolated oven. Therefore, the reaction can be considered to be conducted in a homogeneous environment. Its reaction conversion rate α can be represented by the increase of reaction temperature, as shown in the following equation:

$$a = (M_0 - M_t)/M_0 = H_t/H_{tot} = (T - T_0)\Big/\left(T_f - T_0\right) \tag{7}$$

$$\mathrm{d}a/\mathrm{d}t = 1\Big/\left(T_f - T_0\right) \cdot \mathrm{d}T/\mathrm{d}t \tag{8}$$

where M_0 and M_t are the initial reactant concentration and the reactant concentration at reaction time t, respectively; H_{tot} and H_t are total reaction enthalpy and the reaction enthalpy at reaction time t, respectively; T_0, T_f and T are the initial reaction temperature, final reaction temperature and reaction temperature at reaction time t, respectively. Finally, the Equation (9) was obtained after combining Equations (6)–(8), as shown as following:

$$\ln\left[1\Big/\left(T_f - T_0\right) \cdot \mathrm{d}T/\mathrm{d}t\right] = \ln A + n \cdot \ln\left[1 - (T - T_0)\Big/T_f - T_0\right] - E/RT \tag{9}$$

Calculating Equation (9) at different temperatures, and the reaction kinetics parameters can be obtained, as shown in Table 1. The apparent activation energy E and pre-exponential factor A increased, indicating that the polymerization reaction became difficult with the increase of POD content. TDI-POD macro-initiator showed low reactivity due to the steric effect of multi-armed long-chain structure. The reaction order n of neat nylon-6 and the copolymers with low POD content (1.5 wt%) were approximated to 1, indicating of the one-step reaction, while the reaction process of

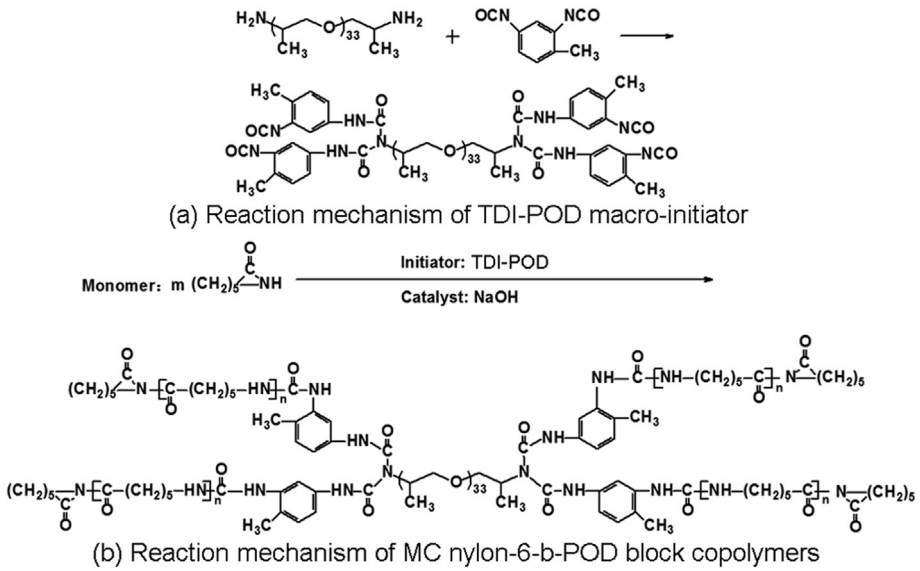

Scheme 1. Reaction process of TDI-POD macro-initiator and MC nylon-6-b-POD copolymers.

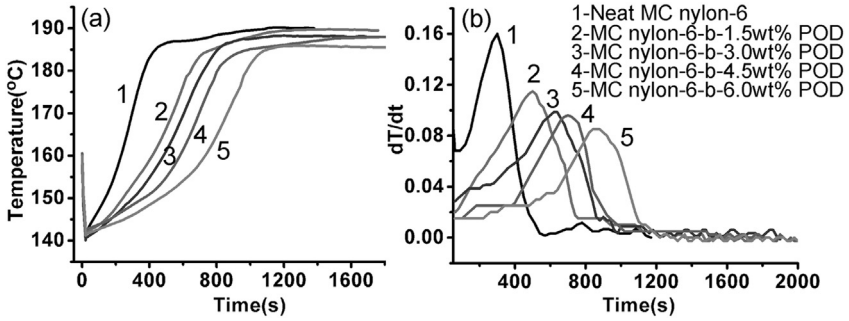

Fig. 1. Temperature–time relationship curves of the synthesis of MC nylon-6-b-POD copolymers.

the MC nylon-6-b-POD copolymers with high POD content (3.0–6.0 wt%) were deviated from one-step reaction.

3.1.2. Molecular weight

The molecular weight of MC nylon-6-b-POD copolymers with various POD content obtained by viscosity method is shown in Table 1. It can be seen that the molecular weight of the copolymers decreased gradually with the increase of POD content, resulting from the decreasing reactivity and reaction rate of the polymerization process by introduction of POD component.

3.1.3. Molecular structure

The structure of MC nylon-6-b-POD copolymers with various POD content was confirmed by the ^{1}H NMR analysis in trifluoroacetic acid-D at room temperature. As shown in Fig. 2, both the ^{1}H NMR spectra of neat MC nylon-6 and MC nylon-6-b-POD copolymers presented the characteristic chemical shift of nylon-6 molecular chains. The three chemical shifts at 1.58 ppm, 1.82 ppm and 1.90 ppm were attributed to the methylene *b*, and the chemical shifts at 2.79 ppm and 3.63 ppm were attributed to the methylene *a* and *c* adjacent to the carbonyl group –C=O and imino group –NH, respectively. The shift at 2.23 ppm was ascribed to the methyl *f* adjacent to benzene. In addition, the copolymers presented a new chemical shift at 1.49 ppm which was due to the methyl *h* adjacent to the methyne –CH in POD molecular chains.

The grafting ratio of MC nylon-6-b-POD copolymers with different dosages of POD can be calculated based on the signal intensities of the aforementioned methylene resonance at 2.79 ppm and methyl peak at 1.49 ppm. The chemical shift at 2.79 ppm of methylene *a* on nylon-6 chain was used as the internal standard and the grafting ratio of POD component can be characterized by the ratio of shift area of methyl *h* and methylene *a* after

Table 1
Reaction kinetics parameters and molecular weight of MC nylon-6-b-POD copolymers.

POD content (wt%)	E (kJ mol^{-1})	A (s^{-1})	n	R_{max} (°C/s)	t_{max} (s)	Molecular weight (g/mol)
0.0	86.27	$5.34*10^7$	0.96	0.154	320	11472.4
1.5	101.04	$1.29*10^9$	1.13	0.115	520	10089.7
3.0	127.84	$8.43*10^{12}$	1.34	0.098	620	93351.4
4.5	143.52	$1.67*10^{13}$	1.57	0.095	700	53108.6
6.0	152.31	$2.68*10^{14}$	1.71	0.085	880	45345.8

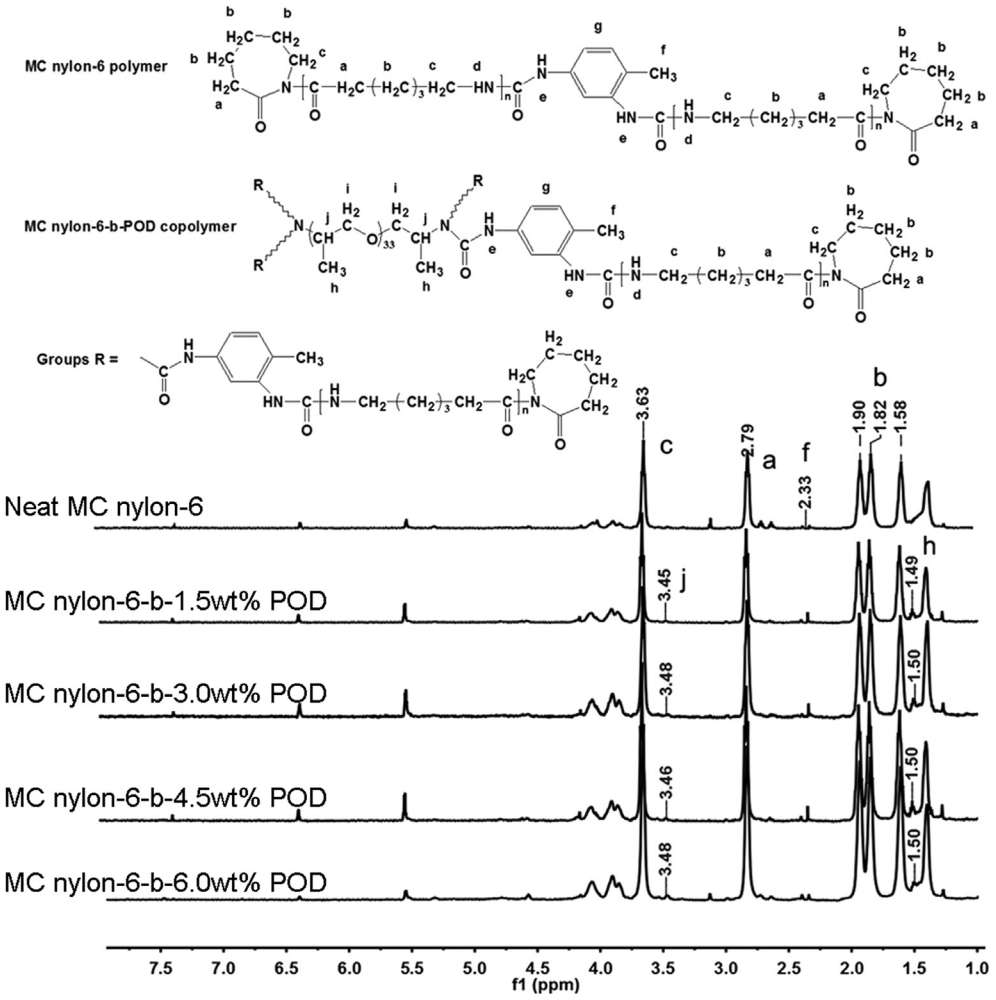

Fig. 2. ^{1}H NMR spectra of MC nylon-6-b-POD copolymers.

copolymerization by the following equation and the results are listed in Table 2.

$$\text{Grafting ratio} = M_{POD}/[M_{POD} + m \times 3 \times H_a \times M_{PA6\ unit}/(2 \times H_h)] \quad (10)$$

where H_a and H_h are the peak areas of the signals at 2.79 ppm and 1.49 ppm, respectively; m and M_{POD} are the repeat unit number and molecular weight of POD segment, respectively; $M_{PA6\ unit}$ is the molecular weight of nylon-6 repeat unit. In this case, m is 34, M_{POD} and $M_{PA6\ unit}$ are equal to 2000 g/mol and 113 g/mol, respectively.

As shown in Table 2, with increasing content of POD, the actual grafting ratio of POD segment increased and was close to the addition content, indicating of the high grafting efficiency of POD component.

3.1.4. Molecular interaction

The FTIR analysis was used to study the inter-molecular forces of multi-branched molecular chains. The FTIR spectra of neat MC nylon-6 and MC nylon-6-b-POD copolymers with various POD content are shown in Fig. 3. As well known, the amide group −NH in nylon-6 matrix presents two different forms which are non-hydrogen-bonded −NH and hydrogen-bonded −NH. Because of

Table 2
Grafting ratio of MC nylon-6-b-POD copolymers.

POD content (wt%)	Type of H	Number of H	δ (ppm)	Integration area Si	Grafting ratio (wt%)
0.0	H_a	2	2.79	67.5	0.00
	H_h	3	1.49	0	
1.5	H_a	2	2.79	63.6	1.46
	H_h	3	1.49	2.74	
3.0	H_a	2	2.79	56.3	2.91
	H_h	3	1.49	4.91	
4.5	H_a	2	2.79	50.6	4.35
	H_h	3	1.49	6.73	
6.0	H_a	2	2.79	45.4	5.82
	H_h	3	1.49	8.25	

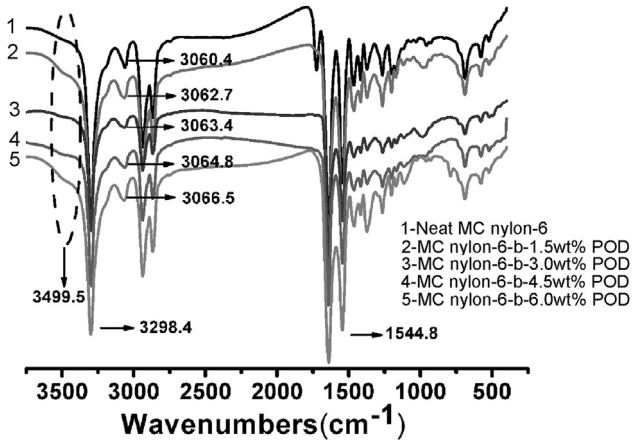

Fig. 3. FTIR spectra of MC nylon-6-b-POD copolymers.

the large number of amide group −NH and carbonyl group −C═O in nylon-6 molecular chains, there formed large quantity of hydrogen bonds in nylon-6 matrix, and the nylon-6 molecular chains were tightly linked and formed orderly crystalline region. The rest small amount of amide group presented as non-hydrogen-bonded −NH in the disorderly amorphous region.

As seen in Fig. 3, compared with neat nylon-6, the FTIR peak at 3298.4 cm^{-1} for the copolymers corresponding to the hydrogen-bonded −NH had no significant change. However, the copolymers showed a new peak at 3499.5 cm^{-1} which was attributed to the non-hydrogen-bonded −NH. Additional, as reported, the absorption peak at 1544.8 cm^{-1} was attributed to the amide II vibration mode and the absorption peak at 3060.4 cm^{-1} was attributed to the octave of amide II, which blue shifted to 3066.5 cm^{-1} gradually with the increase of POD content, indicating that the number of free amide group of the copolymer increased. The result of FTIR revealed that the amide group in neat nylon-6 almost presented as hydrogen-bonded −NH and the crystallization was relatively perfect, while the hydrogen bond and inter-molecular forces of the copolymers were weakened by introduction of multi-branched molecular chains.

3.2. Crystallization properties of MC nylon-6-b-POD copolymers

3.2.1. Crystallization behavior

The non-isothermal DSC curves of neat MC nylon-6 and MC nylon-6-b-POD copolymers with various POD content at a heating and cooling rate of 10 °C/min are shown in Fig. 4, from which the crystallization peak temperature (T_c), the melting temperature (T_m), the half peak width (ΔW) and the crystallinity ($X_{c,\ DSC}$) can be obtained, as listed in Table 3.

The melting process presented only one melting peak in the temperature range of 200–220 °C which corresponded to the melting peak of nylon-6 matrix for all samples. This indicated that the POD segments, incorporated into the nylon-6 main chains, were in the amorphous state. This result revealed the semi-crystalline character of nylon-6 and the completely amorphous character of POD segments in the copolymers. The soft segments did not crystallize whatever their contents.

As listed in Table 3, it can be seen that the introduction of POD led to an obviously decrease of the melting and crystallization temperature, and crystallinity of the MC nylon-6-b-POD copolymers. The increase of half peak width indicated the decrease of crystalline growth rate.

3.2.2. Crystal structure

X-ray diffraction (XRD) analysis was performed to evaluate the crystal structure of neat MC nylon-6 and MC nylon-6-b-POD copolymers. As shown in Fig. 5, for all the samples, the observed diffractions at $2\theta = 20°$ and $23°$ corresponded to α crystalline form of nylon-6 matrix and were indexed as (200) and (002/202) reflections respectively [16,17]. XRD pattern of the MC nylon-6-b-POD copolymers exhibited similar diffraction peaks compared with that of neat MC nylon-6 except the copolymer with 6.0 wt% POD content in which a new and small diffraction peak at $2\theta = 11.58°$ was observed. This diffraction peak at $2\theta = 11.58°$ was also found by other researchers in the polymer system based on nylon-6 matrix [18,19], which was attributed to the γ crystalline form and indexed as (020) reflection. The γ-form was constituted by nylon-6 molecular chains adopting the parallel chain arrangement of hydrogen bonds and the hydrogen bonds sheet was suberect to the carbon skeleton sheet, whereas the nylon-6 molecular chains in the α-form have taken the more stable anti-parallel chain arrangement of hydrogen bonds and the hydrogen bonds sheet was parallel with the carbon skeleton sheet. The α-form was more stable than γ-form because of the shorter hydrogen bonds [20]. Generally, the orderly arrangement of nylon-6 molecular chains was beneficial for the formation of α-form with short and strong hydrogen bonds while the disorderly arrangement of multi-branched nylon-6 molecular chains was in favor of the formation of γ-form with long and weak hydrogen bonds. Therefore, the γ-form of the MC nylon-6-b-POD copolymer with 6.0 wt% POD content at $2\theta = 11.58°$ probably formed due to the disorderly arrangement of multi-branched copolymer molecular chains. Besides, the peak shape and location of α-form had no notable change suggesting that the crystallization of MC nylon-6-b-POD copolymers mainly conducted in α-form and gradually formed a small amount of γ-form simultaneously when the POD content was added up to 6.0 wt%.

The crystallinity ($X_{c,\ XRD}$) and crystal grain sizes were given with the following expressions, respectively:

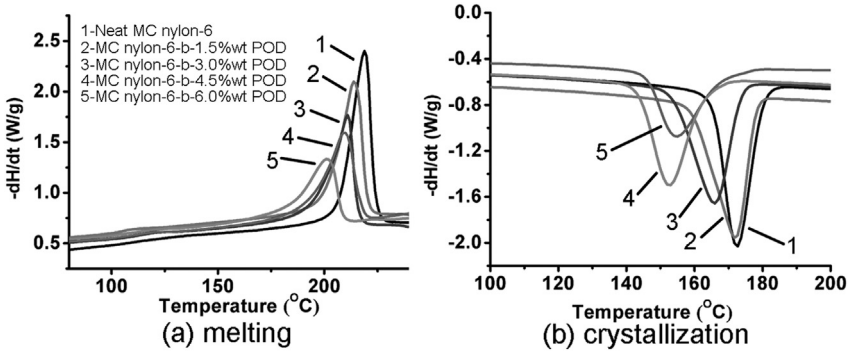

Fig. 4. Non-isothermal process of MC nylon-6-b-POD copolymers.

Table 3
Non-isothermal DSC parameters of MC nylon-6-b-POD copolymers.

POD content (wt%)	T_m (°C)	T_c (°C)	ΔW (°C)	ΔH_m (J/g)	$X_{c,\ DSC}$ (%)
0.0	219.0	172.4	9.8	109.9	47.78
1.5	214.1	171.0	10.6	97.33	42.32
3.0	211.1	165.8	11.3	80.93	35.19
4.5	209.5	154.7	13.7	77.87	33.86
6.0	201.4	152.5	15.3	65.69	28.56

$$X_{c,XRD} = [I_c/(I_c + I_a)] \times 100\% \tag{11}$$

where I_c is the area under the crystalline curve and I_a is the area under the amorphous curve.

$$\text{Scherrer formula} \quad L_{hlk} = k\lambda/(\beta \cos\theta) \tag{12}$$

where the variable L_{hlk} is the size of crystallites from normal direction of *hlk* plane; k is Scherrer constant ($k = 0.9$); λ is radiation wave length, equal to *0.154 nm* in the present case and β is the full width of half maximum of the diffraction peak (*hlk*); θ is Bragg angle.

As shown in Table 4, the crystallinity and crystal grain size of nylon-6 matrix decreased gradually by introduction of POD component which was coincident with DSC analysis.

The spherulite morphology images of neat MC nylon-6 and MC nylon-6-b-POD copolymers obtained by PLM (polarized light microscopy) are shown in Fig. 6. It was concluded by the DSC analysis and XRD analysis that the POD component did not crystallized individually. Therefore, the spherulites observed by PLM were attributed to nylon-6 matrix completely. Compared with the neat MC nylon-6 sample, the spherulite size of the MC nylon-6-b-POD copolymers decreased significantly after introducing POD component.

It was well known that the small spherulite was better for toughness than big one. Therefore, in one aspect, the decrease of spherulite size of the MC nylon-6-b-POD copolymers was beneficial for the improvement of impact strength.

3.3. Rheological behavior of MC nylon-6-b-POD copolymers

The molecular chain entanglement behavior of the neat MC nylon-6 and MC nylon-6-b-POD copolymers was investigated by dynamical rheological measurement. As shown in Fig. 7(a), the complex viscosity as a function of frequency, a pseudo-plastic fluid characteristic of nylon-6 flow behavior was observed. With the increase of POD content, the copolymers presented more and more

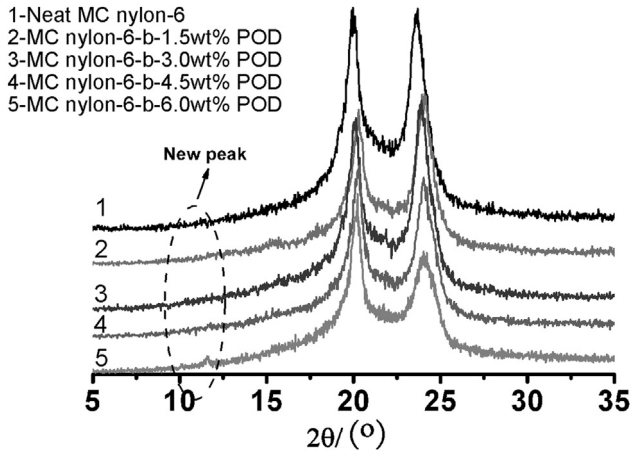

Fig. 5. XRD spectra of MC nylon-6-b-POD copolymers.

Table 4
XRD parameters of MC nylon-6-b-POD copolymers.

POD content (wt%)	Angle (2θ)			$X_{c,\ XRD}$ (%)	Grain size (Å)
	a_1 (°)	a_2 (°)	γ (°)		
0.0	20.14	23.60		36.86	86
1.5	20.29	23.91		33.42	84
3.0	20.09	23.87		31.10	79
4.5	20.34	23.75		28.18	76
6.0	20.27	23.53	11.58	25.48	72

characteristic of shear-thinning. The difference in complex viscosity between neat MC nylon-6 and MC nylon-6-b-POD copolymers may be closely related to the multi-branched molecular chain structure of copolymers. The physical entanglement of molecular chains of MC nylon-6-b-POD copolymers was significant and strong due to the large quantity of long-branched molecular chains. In the low frequency region, the disentanglement process was difficult and slow, and the copolymers showed higher complex viscosity than that of neat nylon-6. As the frequency rise, the physical entanglement point was destroyed significantly and the fluid resistance decreased, and the copolymers showed lower complex viscosity than that of neat nylon-6.

The multi-branched molecular chain also caused a dramatic increase in elastic modulus (G′) and viscous modulus (G″) of MC nylon-6. The linear viscoelastic moduli of the neat MC nylon-6 and MC nylon-6-b-POD copolymers are shown in Fig. 7(b,c) as a function of frequency. As seen in Fig. 7, for all samples, both the elastic modulus and viscous modulus increased with the increase of frequency. Besides, to compare the samples at the same frequency, it can be seen that the viscoelastic moduli of MC nylon-6-b-POD copolymers were higher than that of neat MC nylon-6, and the viscoelastic moduli increased gradually with the increase of POD content. This result was probably due to the severe entanglement through the formation of physical networks with large quantity of multi-branched molecular chains.

The Carreau equation [21] can be applied to investigate the effect of multi-branched long chain on the rheological parameters of nylon-6, which is written as:

$$\eta = \eta_0 \Big/ \left[1 + (\lambda\omega)^2\right]^{(1-n)/2} \tag{13}$$

where η and η_0 are complex viscosity and zero shear viscosity, respectively; ω is the shear frequency; λ is the relaxation time whose reciprocal accounts for the onset of shear-thinning region and n is the shear-thinning index.

By fitting the experimental data with the Carreau equation, the rheological parameters η_0, λ and n were obtained and listed in Table 5. It can be seen that η_0 and λ increased gradually with the increase of POD content which further confirmed the much more entanglement of multi-branched molecular chain of the copolymers than that of neat nylon-6.

The entanglement molecular weight M_e is introduced from the kinetic theory of rubber elasticity. It can be calculated from the plateau modulus and interprets as the apparent average molecular weight between coupling junction. The calculations of entanglement molecular weight M_e and plateau modulus G_N^0 were shown as following respectively.

$$M_e = \rho RT \Big/ G_N^0 \tag{14}$$

$$G_N^0 = (2/\pi) \int_{-\infty}^{+\infty} G''(\omega) \mathrm{d}\ln\omega \tag{15}$$

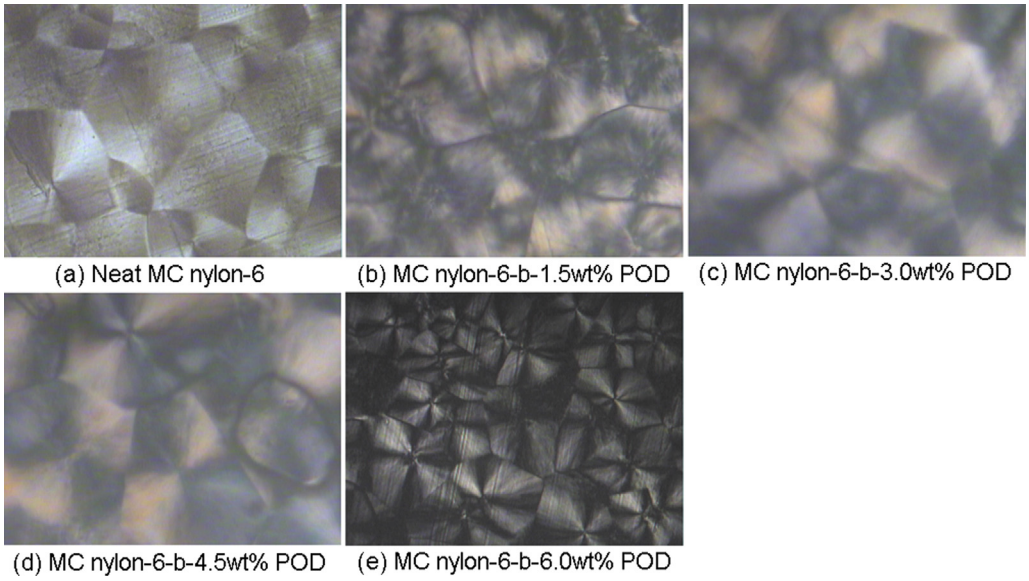

Fig. 6. Spherulite morphology of MC nylon-6-b-POD copolymers (magnification: ×500).

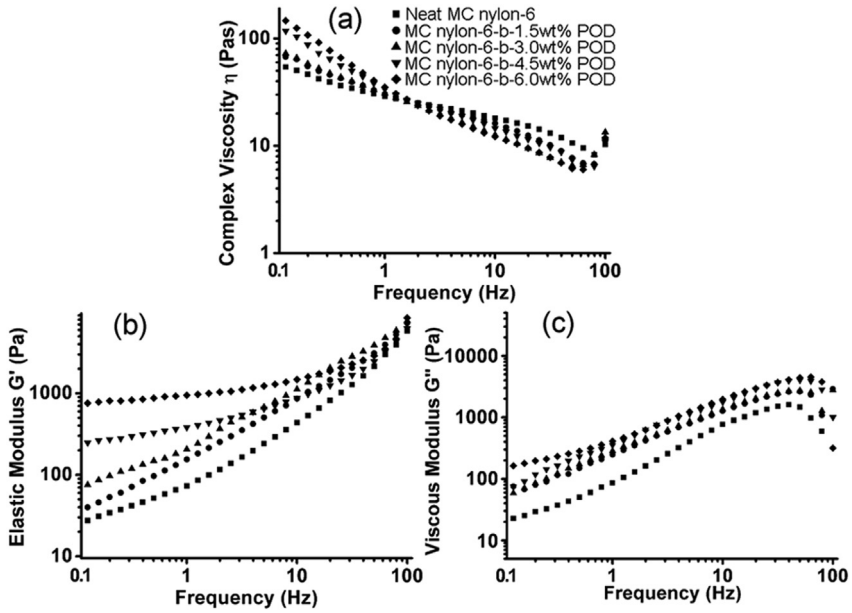

Fig. 7. Rheological behavior of MC nylon-6-b-POD copolymers.

Considering the influence of chain-sliding on entanglement network structure, Doi-Edwards proposed the reptation model and revised the equation as follows:

$$M_e = (4/5)\rho RT \Big/ G_N^0 \tag{16}$$

And the entanglement density ν_e can be calculated by the equation as follows:

$$\nu_e = \rho / M_e \tag{17}$$

Table 5
Rheological parameters of MC nylon-6-b-POD copolymers.

POD content (wt%)	λ (s)	n	η_0 (Pa s)	G_N^0 (Pa)	ν_e (mol/m^3)	M_e (g/mol)
0.0	13.25	0.73	61.54	3173.16	0.92	1,228,153
1.5	64.66	0.68	139.11	6469.96	1.86	602,341
3.0	73.31	0.60	171.28	6869.72	1.97	567,290
4.5	97.72	0.49	403.99	9588.89	2.76	406,421
6.0	106.55	0.50	430.16	11819.73	3.40	329,713

where ρ is the polymer density; R is gas constant; T is the absolute temperature and G_N^0 is the plateau modulus.

The entanglement molecular weight and entanglement density of the neat MC nylon-6 and MC nylon-6-b-POD copolymers were listed in Table 5. It can be seen that the entanglement density increased gradually and the entanglement molecular weight decreased gradually with increasing POD content.

3.4. Mechanical properties of MC nylon-6-b-POD copolymers

3.4.1. Static mechanical properties

Fig. 8(a) shows the tensile stress-strain curves of neat MC nylon-6 and MC nylon-6-b-POD copolymers. It can be seen that the stress-strain curves of the neat MC nylon-6 and the copolymer with 1.5 wt % POD content presented a typical yield point and an unobvious elastic deformation stress plateau. And these two samples showed a high strength and low elongation at break. With the further increase of POD content, the area under stress-strain curves increased dramatically compared with that of neat MC nylon-6, indicating of significantly increasing toughness of MC nylon-6-b-POD copolymers. Moreover, the copolymers with high POD content (3.0–6.0 wt%) presented a special stress-strain behavior: the stress-strain curves showed an untypical yield point and presented an obvious strain hardening behavior after a long elastic deformation stress plateau.

Fig. 8(b, c) shows the mechanical properties of MC nylon-6-b-POD copolymers with various POD content and the experimental errors were listed in Table 6. It can be seen that the elongation at break and notched impact strength of the copolymers were dramatically higher than that of neat MC nylon-6, indicating of the notable toughening effect of POD on the nylon-6 matrix, while the tensile strength of the copolymers decreased gradually with the increase of POD content.

3.4.2. Dynamical mechanical analysis

The dynamical mechanical properties of neat MC nylon-6 and MC nylon-6-b-POD copolymers with various POD content are shown in Fig. 9 and the numerical DMA data are listed in Table 7. It can be seen that the storage modulus of the copolymers dramatically decreased by introduction of POD soft component. The tan δ curve of neat MC nylon-6 showed two relaxation peaks at about −60 °C and 54 °C corresponding to the β relaxation and α relaxation, respectively. The α relaxation aroused by chain segmental motion of molecules in the amorphous region and corresponded to the glass transition temperature (T_g). The high glass transition temperature of neat MC nylon-6 indicated the rigidity of the neat MC nylon-6 molecular chains. In the case of MC nylon-6-b-POD copolymers, the α relaxation peak shifted to low temperature dramatically by introduction of POD soft component while the change of β relaxation was not obvious.

The values of loss factor of MC nylon-6-b-POD copolymers were also improved significantly compared with that of neat MC nylon-6, and increased gradually with POD content, which indicated that the movement of copolymers molecular chains was easy and the internal friction increased by the introduction of multi-branched molecular chain.

3.5. Toughening mechanism

To understand the relationship between the properties and the phase morphology of the copolymers, it is necessary to study the fracture surface morphology of the copolymers by using SEM technology.

Fig. 10(a) shows a cryogenically fracture surface of the MC nylon-6-b-POD copolymers with 6.0 wt% POD content, in which a very smooth and uniform cryogenically fracture surface morphology was observed. It was impossible to distinguish the interface between the two phases, which suggested that MC nylon-6 phase and POD phase were compatible. POD component are covalently connected with nylon-6 molecules and phase separation in excess of a micrometer scale between the two components was difficult. This conclusion was also confirmed by the presence of only one glass transition temperature of DMA analysis.

The micrograph of impact fracture surface of the MC nylon-6-b-POD copolymers with various POD content was observed at low magnification (×500) and high magnification (×5000),

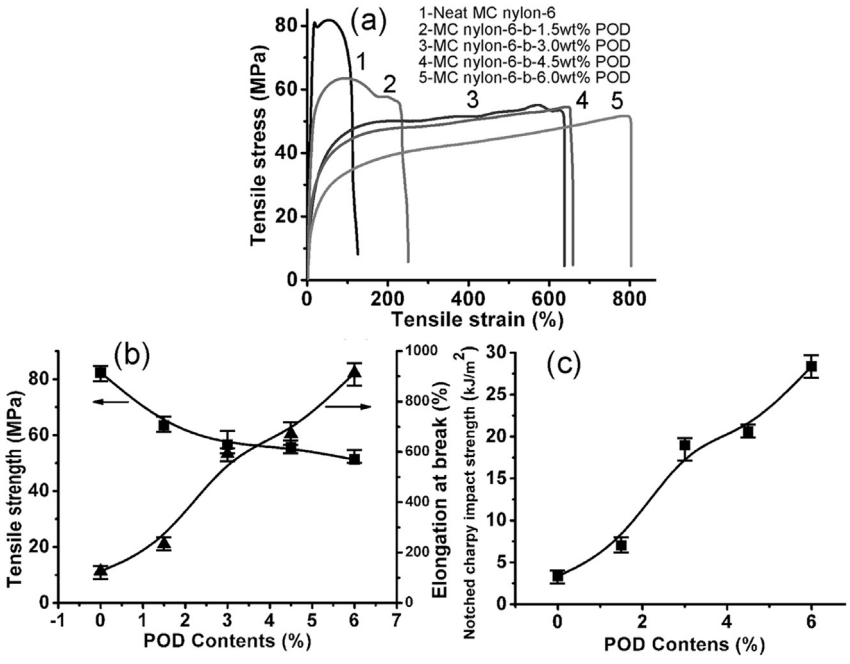

Fig. 8. Mechanical properties of MC nylon-6-b-POD copolymers.

Table 6
Experimental errors of mechanical parameters for MC nylon-6-b-POD copolymers.

POD content (wt%)	Tensile strength (MPa)		Notched impact strength (kJ/m^2)		Elongation at break (%)	
	Average value	SD	Average value	SD	Average value	SD
0.0	82.37	0.96	3.34	0.82	125.78	10.77
1.5	63.54	0.35	7.00	0.73	233.65	14.75
3.0	56.61	0.47	18.95	0.61	591.67	18.23
4.5	55.56	0.98	20.58	0.71	671.40	11.16
6.0	51.22	0.42	28.37	0.48	913.43	22.09

Note: SD represents the standard deviation.

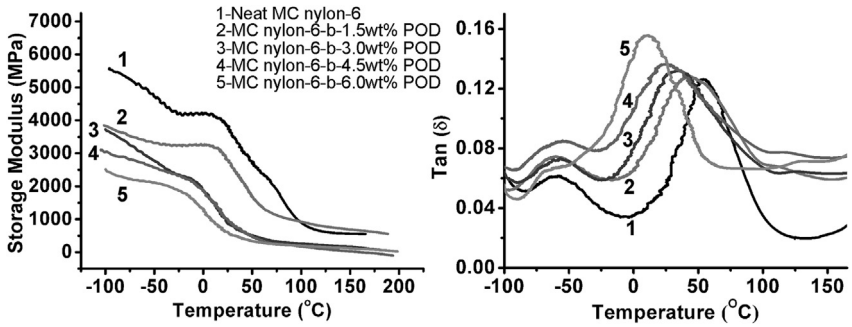

Fig. 9. Dynamic mechanical properties of MC nylon-6-b-POD copolymers.

Table 7
Numerical DMA data of MC nylon-6-b-POD copolymers.

POD content (wt%)	Storage modulus (MPa)	α Relaxation temperature (°C)	β Relaxation temperature (°C)	Loss factor tan δ
0.0	5466	54.0	−60.5	0.1263
1.5	3849	44.9	−60.4	0.1280
3.0	3729	33.6	−61.5	0.1322
4.5	3111	24.9	−58.8	0.1365
6.0	2512	11.4	−59.7	0.1557

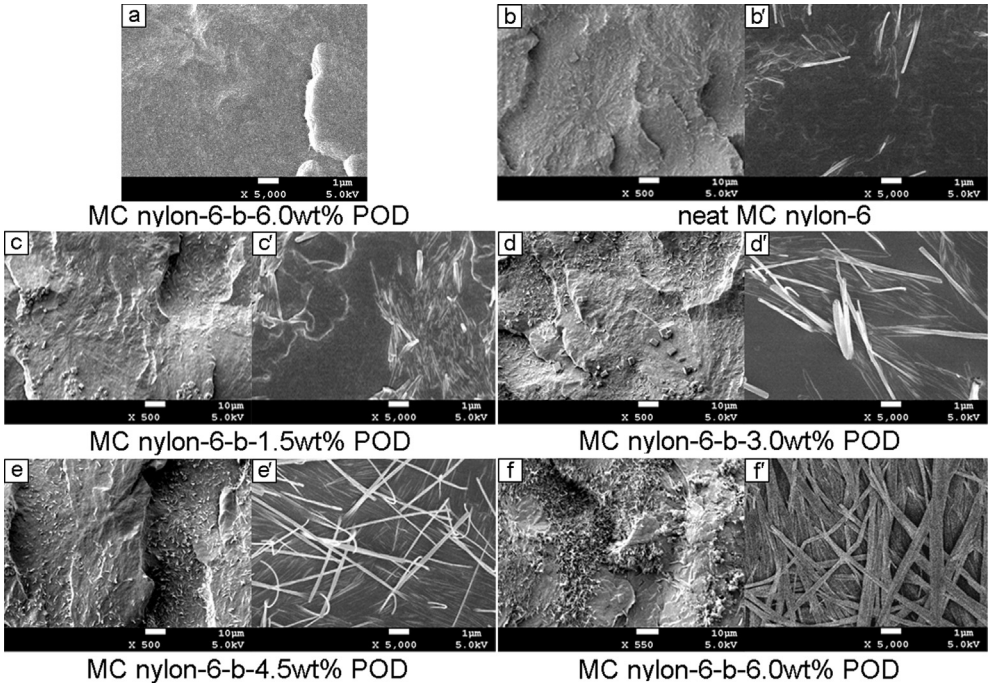

Fig. 10. SEM image of cryogenically fracture surface (a: magnification ×5000) and impact fracture surface of MC nylon-6-b-POD copolymers (b–f: magnification ×500; b′–f′: magnification ×5000).

respectively. As seen in Fig. 10(b)–(f) at low magnification (×500), the fracture surface of neat MC nylon-6 was relatively smooth and partly covered with striations, and showed a typical brittle fracture. By introduction of POD component, the fracture surface of copolymers changed from few small striations to many big striations and became rough. Many yield folds appeared and accompanied by a large number of major deformation by absorbing impact energy with the increase of POD content, displaying character of tough fracture. A hairy structure was observed on the fracture surface of the copolymers and this phenomenon became evident with the increase of POD content. The fracture surface of the neat MC nylon-6 and MC nylon-b-POD copolymer was further observed at high magnification (×5000), as seen in Fig. 10(b′)–(f′), the hairy structure on fracture surface was acicular fiber of the nylon-6 matrix actually which was formed by the way similar to wire-drawing of the matrix under shear stress. As shown in Fig. 11, it can be seen that the distribution of both the fiber length and fiber diameter was relatively concentrated as to the certain copolymer. To compare the fiber's morphology of different copolymers, it can be seen that the fiber length became longer and the fiber diameter became larger dramatically with the increase of POD content.

Some classic theories were proposed by researchers, such as Merz's micro-crack toughening theory; Bucknall's multiple crazing theory and craze-shear band theory; Newman's shear yielding theory and Bascom's hole theory et al. In this work, as seen in Fig. 10, after being suffered with shear stress, many acicular fibers formed on the impact fracture surface of the samples and the fibers were connected to the matrix resin. The front part of the acicular fibers showed whitening phenomenon while the bottom part adjacent to the matrix resin was relatively dark. The toughening mechanism of this copolymer system can be deduced to accord with the multi-layer crack extension mechanism. The toughening mechanism was simulated and divided into five steps, as shown in Fig. 12. Step one, there existed certain stress defects in the nylon-6 matrix, which induced the formation of multi-layer micro-crack as the stress concentration points; Step two, these micro-cracks quickly developed into deep micro-crack vacuum layer field with face to face adhesive sheet film; Step three, the adhesive sheet film in micro-crack vacuum layer field was further extended and formed big vacuum region; Step four, under the force of shear stress, the molecular chain of adhesive sheet film oriented intensively along the orientation of the stress and then adhesive sheet film developed to oriented-long fiber; Step five, when the impact energy was higher than the surface energy and the molecular orientation energy after fully extension, the oriented-long fiber broke. The observed whitening phenomenon in the front part of the fibers was closely due to the intensive orientation of fibers under shear stress. Therefore, different from the usual craze-shear band mechanism, the super toughening break of MC nylon-6-b-POD copolymers was based on the energy consumption of the extension of quantity of adhesive sheet films and the orientation of molecular chain or segment in the matrix fibers, not only the result of energy consumption of craze-shear band.

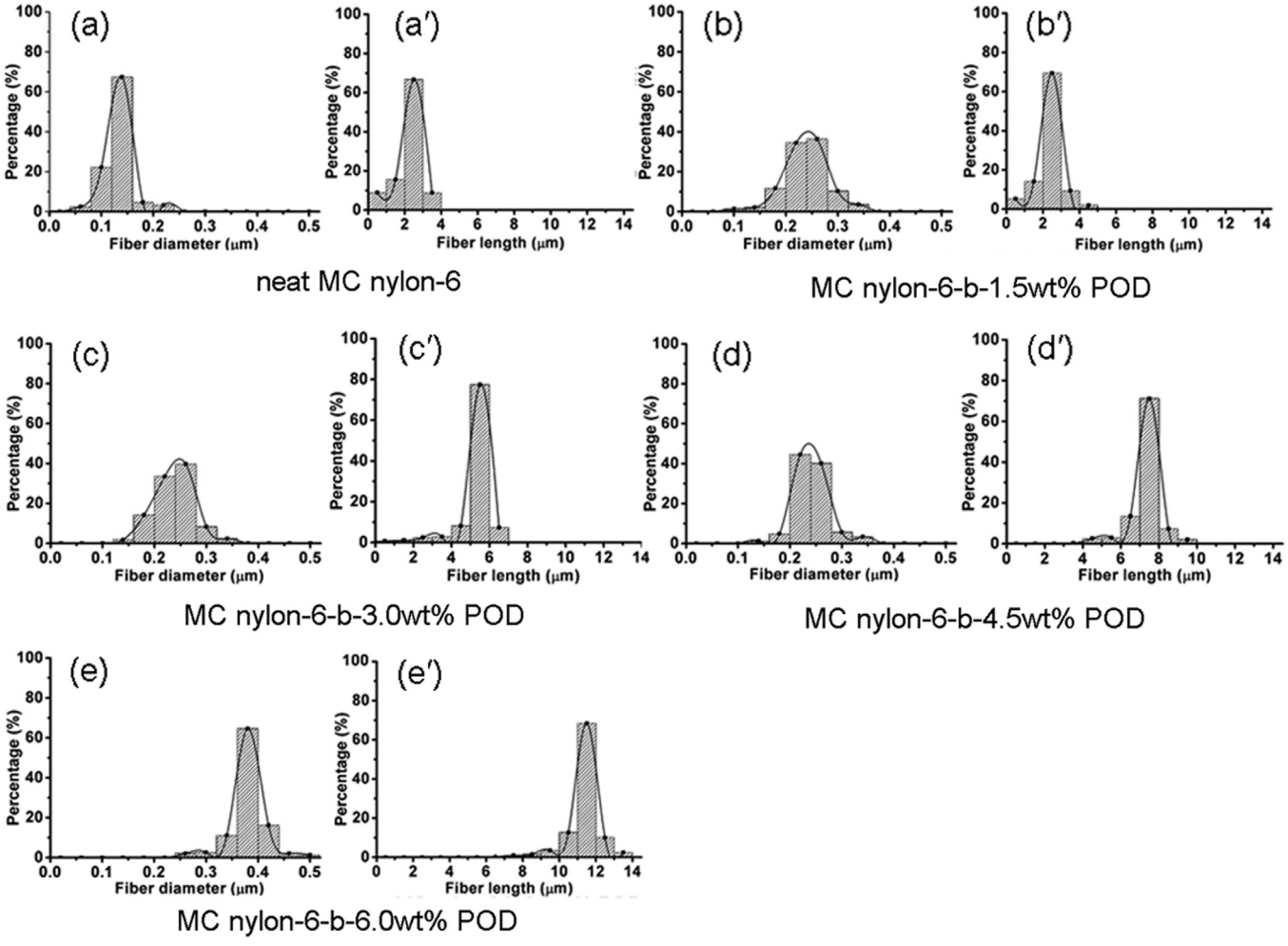

Fig. 11. Distribution of the fiber diameter (a–e) and fiber length (a′–e′) of the MC nylon-6-b-POD copolymers.

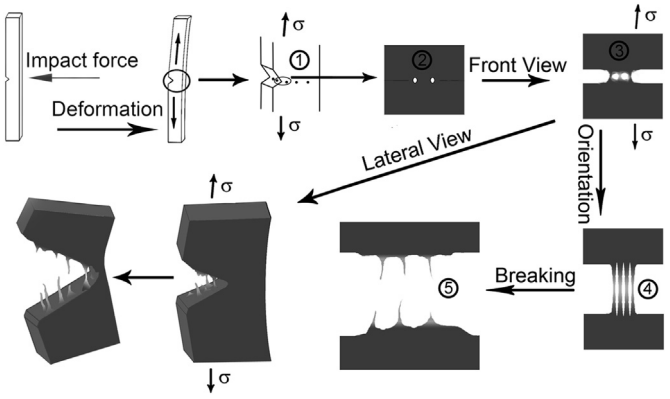

Fig. 12. Toughening mechanism simulation of the MC nylon-6-b-POD copolymers.

Based on the above analysis, the toughening mechanism of MC nylon-6-b-POD copolymers was deduced. On the one hand, the motion of molecular chain of the copolymers was easy because of the decreased hydrogen bonds and weakened inter-molecular forces, which effectively prohibited the crack propagation when the copolymer was suffered with external force. On the other hand, the physical entanglement of molecular chains of the copolymers was significant and strong which increased the entanglement density due to the large quantity of long-branched molecular chains. Moreover, the decrease of crystallinity and spherulite size of the copolymers, and the formation of γ crystalline form with disorderly arrangement of molecular chains also played a positive effect on improving toughness. The large energy consumption caused by hairy structure observed on the fracture surface indicated the multi-layer crack extension mechanism for MC nylon-6-b-POD copolymers.

4. Conclusions

A series of MC nylon-6-b-POD copolymers were prepared via in-situ polymerization. The result showed that the introduction of POD dramatically delayed the polymerization process of caprolactam. The apparent activation energy E and pre-exponential factor A increased, indicating of the lower reactivity of the long-chain macro-initiator than TDI, resulting in the decrease of molecular weight of nylon-6. ^{1}H NMR spectrum characterized the chemical composition and structure of MC nylon-6-b-POD copolymers and FTIR analysis revealed the decrease of hydrogen bonding and weakening of inter-molecular forces of copolymers. DSC and XRD test indicated that the introduction of POD soft component led to a decrease of the crystallization ability of the nylon-6 matrix by reducing crystal grain size and crystallinity. Besides, the crystallization of copolymers was only attributed to the nylon-6 phase and the crystallization of copolymers conducted in α-form mainly and gradually formed a small amount of γ-form simultaneously when the POD content was added up to 6.0 wt%. Dynamic rheology analysis revealed the increasing entanglement of multi-branched long-chain. The increase of entanglement density of copolymers led to a higher viscoelastic moduli and complex viscosity than neat nylon-6. The stress-strain curves of the copolymers presented a typical strain-hardening behavior following with a long elastic deformation stress plateau, indicating of increasing toughness of the copolymers. Dynamical mechanical analysis showed a significant decrease in glass transition temperature, storage module and a dramatically increase in loss factor of the copolymers compared with neat nylon-6, indicating of improved movement of molecular chain segment of copolymers. A hairy structure was observed on the fracture surface of the copolymers and this phenomenon became evidently with the increase of POD content. The toughening mechanism of the copolymers was deduced and corresponded to the multi-layer crack extension mechanism.

References

[1] Zhou FJ, Zhang LQ, Wang YM. Synthesis of MC nylon. Synth Technol Appl 2012;27(2):1–6.
[2] Li F, Zhang JS, Qiu GX. Study on the properties of monomer cast nylon modified by block copolymerized polybutadiene. Eng Plast Appl 2012;40(6):17–20.
[3] Pan BL, Zhang SP, Li WZ, Zhao J, Liu JL, Zhang YQ, et al. Tribological and mechanical investigation of MC nylon reinforced by modified graphene oxide. Wear 2012;294(7):395–401.
[4] Wang W, Meng LH, Huang YD. Hydrolytic degradation of monomer casting nylon in subcritical water. Polym Degrad Stab 2014;110(12):31–317.
[5] Lin X, Zhang PN, Yin ZL, Chen QY. Study on preparation and properties of La_2O_3/MC nylon nanocomposites. J Rare Earths 2005;23(6):680–4.
[6] Zhang YM, Wu XY, Hong W, Zhang W. Toughening properties of MC nylon with UHMWPE particle. Plastics 2009;38(1):68–9.
[7] Wang XH, Zhang Q, Zhang XB, Han DL. A study of the property characterization of MC copolymerized nylon elastomer. China Plast Ind 1996;24(6):55–8.
[8] Kim KJ, Kim YY, Yoon BS, Yoon KJ. Mechanism and kinetics of adiabatic anionic polymerization of ε-caprolactam in the presence of various activators. J Appl Polym Sci 1995;57(12):1347–57.
[9] Van der Schuur MJ, Gaymans RJ. Influence of morphology on the properties of segmented block copolymers. Polymer 2007;48(7):1998–2006.
[10] Cheng XC, Gu X, Zhang QH. Preparation and DSC analyses of MC nylon modified by copolymerization. Appl Chem Ind 2005;34(5):282–4.
[11] Petrov P, Jankova K, Mateva R. Polyamide-6-b-polybutadiene block copolymers: synthesis and properties. J Appl Polym Sci 2003;89(3):711–7.
[12] Ji YL, Ma JH, Liang BR. In situ polymerization and in situ compatibilization of polymer blends of poly(2,6-dimethyl-1,4-phenylene oxide) and polyamide 6. Mater Lett 2005;59(2):1997–2000.
[13] Liu CS, Wang Q. Study on structure and properties of polyamide 6/poly propylene blends. J Wuhan Inst Chem Technol 2001;23(3):35–9.
[14] Karsli NG, Aytac A. Tensile and thermomechanical properties of short carbon fiber reinforced polyamide 6 composites. Compos Part B: Eng 2013;51:270–5.
[15] Segatelli MG, Yoshida IVP, Gonçalves MDC. Natural silica fiber as reinforcing filler of nylon 6. Compos Part B: Eng 2010;41(1):98–105.
[16] Lu CH, Yeh PY, Hsu WT. Non-isothermal reaction kinetics of lithium cobalt oxide. J Alloys Compd 2009;476(1):749–54.
[17] Gong L, Yin B, Li LP, Yang MB. Nylon-6/graphene composites modified through polymeric modification of graphene. Compos Part B: Eng 2015;73:49–56.
[18] Boscoletto AB, Trezza G, Andreis B, Milan L, Tavan M, Furlan P. Anionic polyamides modified with poly(oxypropylene) by "one-shot" RIM technology: structural and morphological characterization. Macromolecules 1992;25(21):5752–8.
[19] Ramesh C, Gowd EB. High-temperature X-ray diffraction studies on the crystalline transitions in the α- and γ-forms of nylon-6. Macromolecules 2001;34(10):3308–13.
[20] Ho JC, Wei KH. Induced γ→α crystal transformation in blends of polyamide 6 and liquid crystalline copolyester. Macromolecules 2000;33(14):5181–6.
[21] Carreau PJ. Rheological equations from molecular network theories. Trans Soc Rheology 1972;16(1):99–127.